Fossil fuel emissions have rapidly worsened European heatwaves in just a few decades

Authors

Theodore Keeping, *Centre for Environmental Policy, Imperial College, London, UK*
Clair Barnes, *Centre for Environmental Policy, Imperial College, London, UK*
Ben Clarke, *Centre for Environmental Policy, Imperial College, London, UK*
Claire Bergin, *ICARUS Climate Research Centre, Maynooth University, Maynooth, Ireland*
Izidine Pinto, *Royal Netherlands Meteorological Institute (KNMI), De Bilt, The Netherlands*
Maja Vahlberg, *Red Cross Red Crescent Climate Centre, The Hague, the Netherlands; Swedish Red Cross, Stockholm, Sweden (based in Ubmeje/Umeå, Sweden)*
Carolina Pereira Marghidan, *Red Cross Red Crescent Climate Centre, The Hague, The Netherlands; University of Twente, Enschede, The Netherlands; Royal Netherlands Meteorological Institute (KNMI), De Bilt, The Netherlands*
Emmanuel Raju, *Copenhagen Centre for Disaster Research; Department of Public Health, University of Copenhagen*
Paula Haro, *International Federation of Red Cross and Red Crescent Societies* (*IFRC) Regional Office for Europe, Budapest, Hungary*
Friederike Otto, *Centre for Environmental Policy, Imperial College, London, UK*

Review authors

Nóra Belágyi, *Royal Netherlands Meteorological Institute (KNMI), De Bilt, The Netherlands*
Julie Arrighi, *Red Cross Red Crescent Climate Centre, The Hague, The Netherlands; Global Disaster Preparedness Centre, Washington D.C., USA; Tufts University, Boston, USA (based in New York, USA)*
Sjoukje Philip, *Royal Netherlands Meteorological Institute (KNMI), De Bilt, The Netherlands*
Sarah Kew, *Royal Netherlands Meteorological Institute (KNMI), De Bilt, The Netherlands*

Cite as Keeping, T. et al. (2026): Fossil fuel emissions have rapidly worsened European heatwaves in just a few decades (WWA scientific report No. 85) World Weather Attribution

Main findings

- Heatwaves cause more deaths in Europe than all other natural hazards combined. As temperatures continue to rise, ageing populations, growing prevalence of chronic illness, and uneven access to cooling and heat-resilient housing are increasing vulnerability, placing mounting pressure on health systems.
- Vulnerability to heat has shifted over time, from primarily elderly people living alone to populations facing socioeconomic disadvantage and chronic illness, including homeless people and migrants, highlighting the need for adaptive, equity-focused heat-health policies.
- Over the region studied this heatwave is the most severe ever recorded.
- In 1976, when some of the previous European records were set, the 2026 temperatures would have been virtually impossible to occur in June, while also highly unlikely at any time of the year. In 2003, the first major heatwave of this century, daytime heat like this would still have been very rare, about 10 times less likely than today, while nighttime temperatures such as this June would have been more than a hundred times less likely in 2003.
- Across large parts of Western Europe, June is warming faster than any other month. In addition, daily maximum temperatures are warming faster than night time temperatures, though both are warming much faster than global warming. The hottest daily temperatures are warming at about triple the rate of global warming and night time temperatures at about twice the rate. Many capital cities are experiencing not only their hottest June 3-day period but also the hottest three-day period since 1950, according to the ERA5 dataset. However, due to global warming these temperatures are now no longer unusual during the summer months in many capitals.
- This means that a similar heatwave in June would have been about 3.5°C cooler during the day in 1976 and about 2°C cooler in 2003. The nighttime temperatures would have been about 2.4°C cooler in June 1976 and about 1.3°C cooler in June 2003.
- This June 2026 heatwave occurred under a circulation pattern broadly similar to historical analogues - Southerly Flow. However, a similar circulation pattern now produces significantly hotter temperatures than it did in the mid-20th century because the climate baseline has warmed.
- As the combination of heat and high humidity is especially dangerous for human health, we also analysed Wet Bulb Globe Temperature (WBGT). During this heatwave (18th - 29th June), 45% of European cities are breaking indoor-WBGT thresholds.
- Heat risk is concentrated in cities, where urban heat island effects, ageing building stock, and socioeconomic inequalities combine to intensity exposure. Many homes, schools, transport systems, and energy infrastructure were not designed for prolonged extreme heat, highlighting the urgent need for equitable adaptation, building retrofits, passive cooling measures, and heat-resilient urban design.
- This summer shows that at 1.4°C of global warming, extreme heat is already reaching the limits of our societies' ability to cope. Our analysis here shows that intense heat is increasing rapidly even in living memory, with such events tens to hundreds of times more likely since only 2003 and virtually impossible just 50 years ago. A rapid phase-out of fossil fuels is critical if we are to avoid even higher temperatures and their consequences in the future.

1 Introduction

From the 18th of June 2026 onwards, Western Europe has experienced exceptionally high temperatures due to a persistent high-pressure system. Following a severe heatwave in May, this is already the second heatwave hitting Europe in 2026. The heatwave is affecting large areas of the continent. In France, red heat alerts have been issued across more than half of the country's departments, impacting an estimated 39 million people. Authorities report at least 18 heat-related deaths since the weekend, including two children who were left in a hot car (Reuters, 2026). More than 1,350 schools have been closed (Guardian, 2026). Rare red warnings have been issued across parts of the UK as extreme temperatures threaten to break longstanding June records amid the intense European heatwave. Temperatures surpassed the previous June record of 35.6°C set in 1976. The temperatures are accompanied by high humidity and unusually warm overnight conditions, limiting opportunities for relief and increasing health risks for vulnerable groups (Guardian, 2026). In the Netherlands, the Royal Netherlands Meteorological Institute (KNMI) issued a Code Orange weather warning, indicating a high likelihood of dangerous weather conditions in the southern and central parts of the country from Wednesday, June 24, through to at least Friday, June 26, with temperatures rising to 33-36°C (KNMI, 2026).

Germany, Spain, Portugal and Switzerland are also seeing extreme temperatures, as the heatwave continues to disrupt daily life across Europe. Schools have been forced to close in several countries, while train services in cities including Paris and Brussels have been scaled back to reduce the risk of heat-related breakdowns. Electricity networks are facing growing strain from surging demand for air conditioning and cooling, causing power outages and making it harder for residents to escape the heat (Euronews, 2026; Guardian, 2026).

Heat is considered the most significant climate-related health risk in Europe (EEA, 2024), with thousands of excess heat-related deaths occurring each year. During the extreme summer of 2022, more than 60,000 heat-related deaths were recorded across Europe, with an estimated 56% attributable to anthropogenic climate change (Ballester et al., 2023; Beck et al., 2024). Even in the less extreme summer of 2023, over 47,000 heat-related deaths occurred (Gallo et al., 2024). Globally, an estimated 178,000 deaths were linked to heatwaves in 2023, more than half of which were attributed to climate change, with Europe experiencing the highest mortality burden (Hundessa et al., 2025).

In this study, we draw a comparison with 2003 and 1976, as two illustrative years subject to major heatwave events, and also events within living memory (23 and 50 years ago). The 2003 heatwave was described as the first major "wake up call" for Europe on the impacts of climate change, it killed over 72,000 people – with the biggest impacts in Italy and France (UNDRR, 2020). The 1976 heatwave primarily affected northern Europe (especially the UK) and led to an increase in excess deaths in e.g. Birmingham, England of approximately 20% (Ellis et al., 1980). Beyond mortality, extreme heat increases hospitalisations, worsens chronic illnesses, and disrupts livelihoods and economic activity, particularly in sectors such as construction, transport, tourism, and informal services (World Bank, 2025).

Europe is warming faster than the global average, a trend that has been attributed with high confidence to human-induced climate change (Seneviratne et al., 2021; Quilcaille et al., 2025). Summer temperatures across Western Europe have increased substantially over recent decades (Vautard et al., 2023; Noest et al., 2026), and the frequency and severity of heat-related impacts are expected to increase further with each additional increment of global mean surface temperature (IPCC, 2021). Since the second half of June 2026, Western Europe has experienced exceptionally high temperatures associated with a persistent anticyclonic circulation pattern. This high-pressure system has been characterised by positive geopotential height anomalies (Figure 1) and has promoted the advection of warm air from North Africa into Western Europe through sustained southerly flow. In addition to enhancing warm-air transport, the associated subsidence and reduced cloud cover have increased surface solar radiation, further amplifying near-surface temperatures across the region.

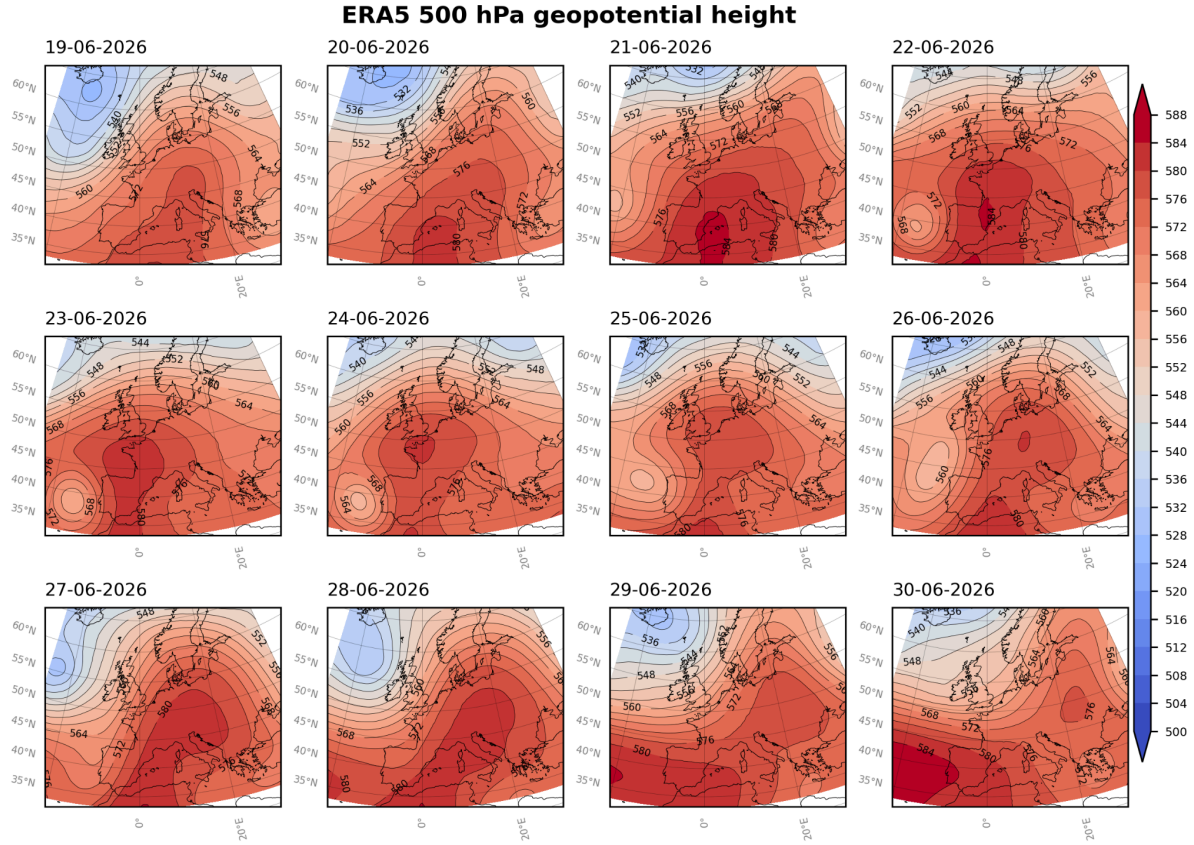

Figure 1: Daily geopotential height at 500 hPa. Data source ERA5.

1.1 Impacts

The Wet Bulb Globe Temperature (WBGT) measures the combined effect of environmental factors on human heat stress, and is used as a composite index, combining humidity, radiant heat (such as direct sunlight), and air movement, all of which affect the body's ability to regulate its internal temperature through sweating and heat exchange. In this study, WBGT was approximated from ERA5 maximum temperature data and dewpoint temperature data (per Zhang et al., 2024) – which means results apply best to a sheltered and shaded area, without the heating effect of direct sunlight or the cooling effect of wind. By capturing the interacting variables, WBGT provides a more physiologically relevant assessment of thermal strain, particularly during outdoor physical activity. Consequently, it is widely applied in fields such as sports science and occupational health (Grundstein et al., 2023).

The WBGT was approximated in this analysis for the same 854 cities across 30 European countries featured in Barnes et al., (2025). It was found that 44.9% of these cities, the locations of which can be seen in Figure 2, experienced their highest-ever WBGT values between 18 and 29 June 2026 as of the 24th of June. All analysed cities in Czechia, Luxembourg and Lithuania are experience record-high WBGT values. Record WBGT conditions were also broken for more than 90% of cities in Germany, the Netherlands, and Poland, and for over 50% of cities in Denmark, Slovakia, Belgium, Ireland, the United Kingdom and Austria. The additional strain placed on the body from high WBGT's is a cause for concern for many members of the public, particularly for more vulnerable members of society.

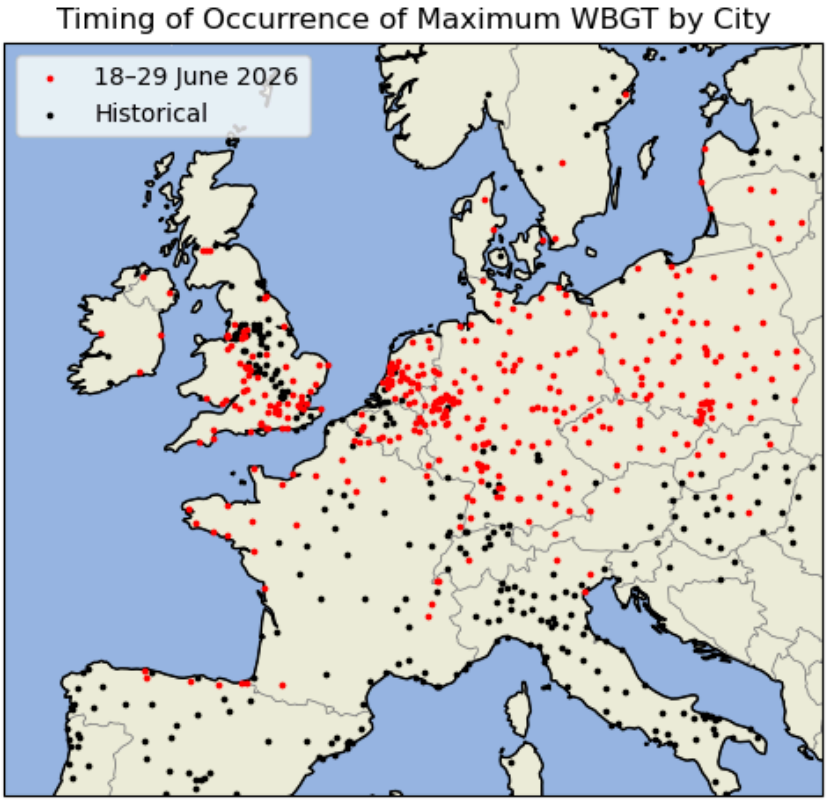

Figure 2: Cities where the highest ever WBGT values observed (or forecast) to occur between 18 and 29 June 2026 are shown in red. The black dots represent cities which do not meet this threshold between 18 and 29 June 2026.

Tropical nights are defined as nights when the minimum temperature does not go below 20°C. They are important from a health perspective, as normally cool night temperatures allow the body to rest and recover from heat stress, with multiple warm nights compounding the body's vulnerability to daytime heat extremes and other health conditions. This has affected regions of Europe that rarely experience these nighttime heat extremes, including the UK, Denmark, northern Germany and Sweden. Nighttime minimum temperatures are understood to have been most severe over France, where in some places temperatures have stayed above 20°C for over a week, with some nights having minimum temperatures of nearly 30°C. Figure 3 shows the area of Europe observed and forecast to be over the 20°C temperature threshold from June 19th-30th 2026.

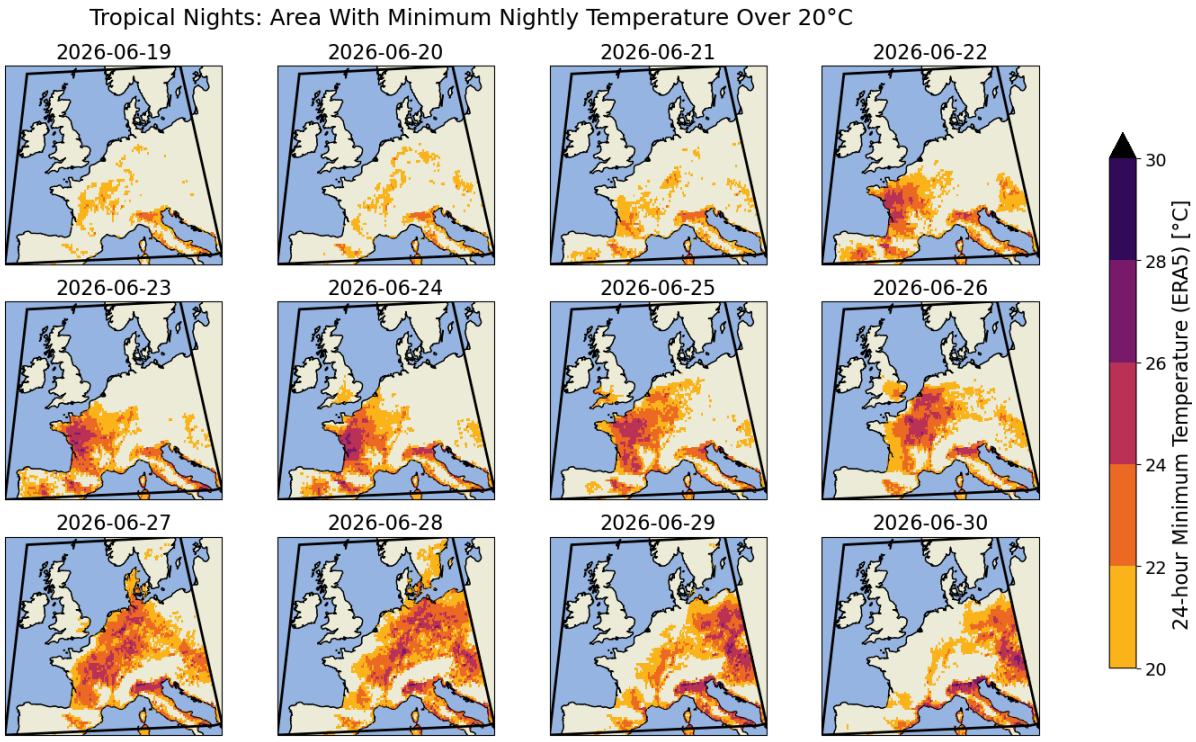

Figure 3: Days with 24-hour minimum temperature exceeding 20°C, per ERA5 analysis (up to 23rd) and forecast (from 24th) data.

1.2 Heat extremes in Europe and anthropogenic climate change

The role of anthropogenic climate change in European summer heatwaves has been extensively studied, with the unequivocal finding that such events are increasing in likelihood and magnitude because of this warming. The first attribution study was on the European summer of 2003, finding that human-induced warming made such a hot summer more than twice as likely (Stott et al., 2004). Since then, numerous major events have occurred that have elicited attribution studies (e.g. Christidis et al., 2015; Vautard et al., 2020; Leach et al., 2020; Zachariah et al., 2022; Feser et al., 2024; Ionita et al., 2024; Barnes et al., 2025). Consistently, such studies have found that heat extremes are warming at a rate much larger than the rate of global warming, and that many recent extreme events would have been very unlikely or virtually impossible without this warming.

These heat extremes continue to be incredibly dangerous. In 2003, more than 70,000 people died because of the exceptionally hot weather and Europe has recorded thousands of excess heat-related deaths each year (Masselot et. al., 2023, Ballester et al., 2023). During the summer of 2022, more than 60,000 people across Europe died as a result of extreme heat (Ballester et al., 2023), and 56% of these excess deaths were directly attributable to human-induced climate change (Beck et al., 2024). A global study recently showed that 178,000 deaths can be linked to heatwaves in 2023 and that more than half (54.29%) of these deaths are attributable to climate change (Hundessa et al., 2025). It also found that the highest mortality rates and excess death ratios occurred in Southern, Eastern and Western Europe, amounting to a total of 66,443 for the continent (Hundessa et al., 2025). Recent work on the heat events of 2025 found that during the summer period, of the 23,500 people who died due to extreme heat in 854 major cities across Europe, more than two-thirds of these (around 16,000) were directly due to the influence of climate change on local temperatures (Barnes et al., 2025). There is,

therefore, a consistent picture across myriad studies that climate change is more than doubling the mortality due to extreme heat events.

Challenges remain in understanding changing heat extremes. First, climate models consistently underestimate trends in heat extremes in Europe. In part, this is known to be due to a failure of models to simulate changes in circulation that favour southerly flows (Vautard et al., 2023); previous studies have found such circulation patterns to be occurring more frequently (Rousi et al., 2022). However, quantifying where and how this underestimation occurs is essential to improve models going forward. Second, in a rapidly warming world, and on an even more rapidly warming continent, more record-breaking and record-shattering extremes are to be expected (Fischer et al., 2021; Fischer et al., 2025). Given the challenge of assessing the present and changing return period of such events (Zeder et al., 2023), it is important that new extreme events are studied using a range of simulation and attribution techniques. This includes new methods such as ensemble-boosting (e.g. Fischer et al., 2023; Suarez-Gutierrez et al., 2026), as well as attribution studies with a range of conditioning levels (Thompson et al., 2025), from more conditioned approaches such as spectrally-nudged storylines (e.g. Feser et al., 2024), to less conditioned probabilistic methods (e.g. Leach et al., 2020; Zachariah et al., 2022). In particular, it is crucial to assess events across spatial and temporal scales, relative rates of change in different parts of the year, and across different heat-related variables that can lead to different impacts. Given these challenges and the known behaviour of models with the type of circulation for this extreme (e.g. Vautard et al., 2020), this study is conducted using observations alone.

1.3 Event Definition

A very large area of Europe has been affected by extreme heat from the period 22nd-30th June 2026. To examine the effect of climate change on extreme heat, we focus on the region bounded by the box 10.5°W to 20°E, and 40 to 60°N. Figure 4 shows the anomaly in maximum daily temperature relative to June daily maximum temperatures in the period 1991-2020, with the bounding box overlaid. Figure 5 shows the equivalent anomaly for daily minimum temperatures. The anomalous heat migrated from west to east, with widespread extreme heat persistent over the study region for more than a week.

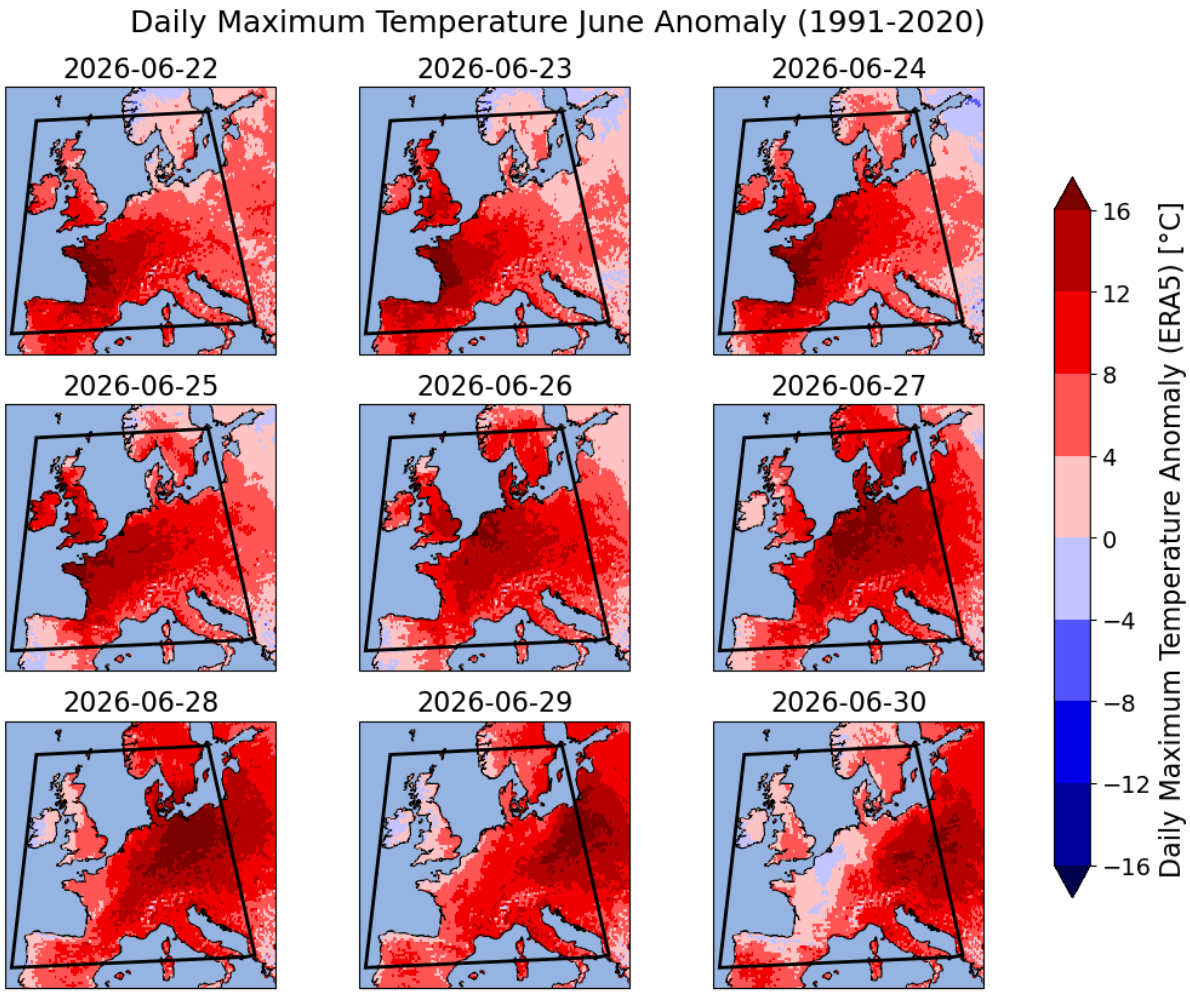

Figure 4: Anomaly of daily maximum temperatures relative to June average from 1991-2020, per ERA5 analysis (up to 23rd) and forecast (from 24th) data.

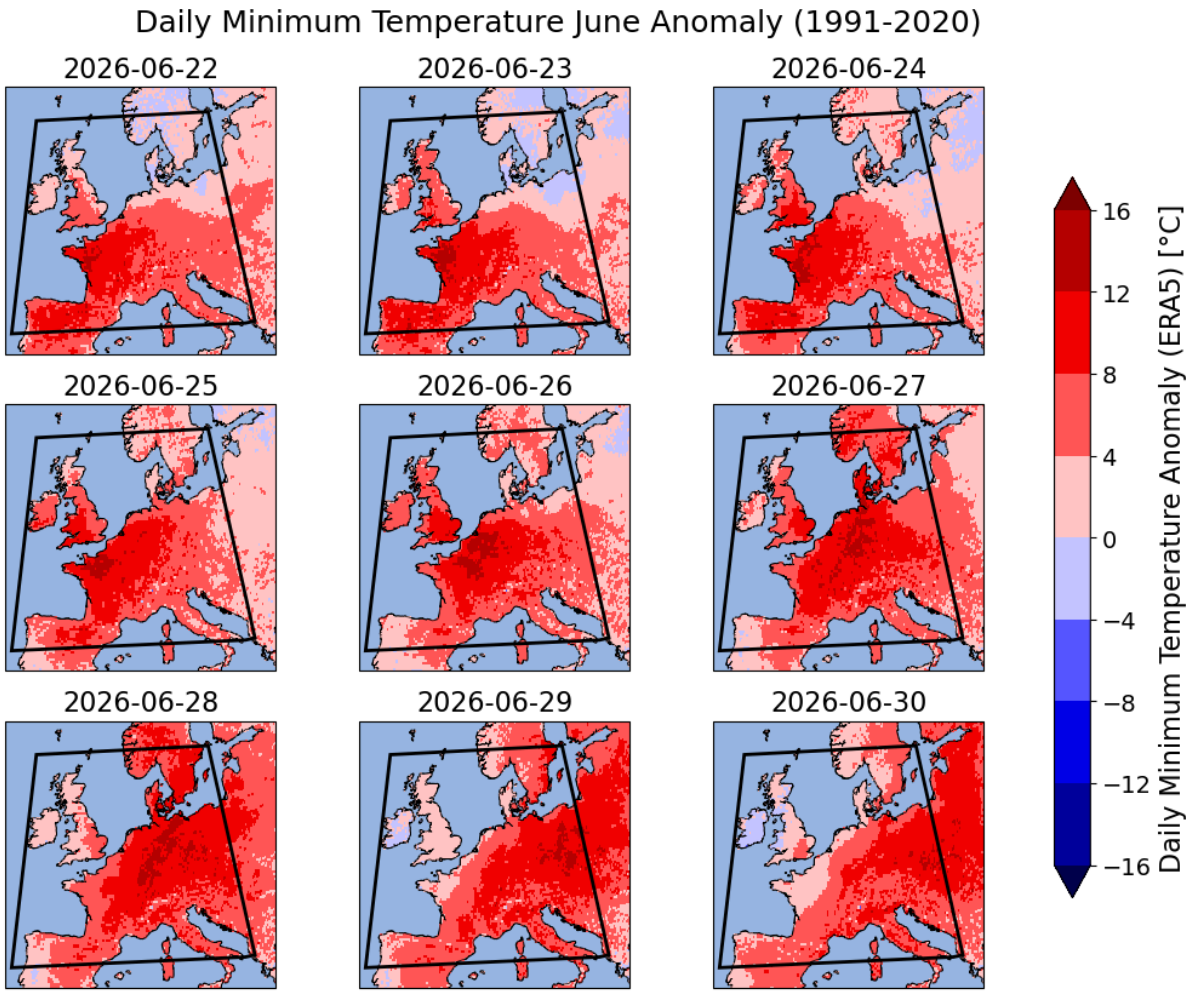

Figure 5: Anomaly of daily minimum temperatures relative to June average from 1991-2020, per ERA5 analysis (up to 23rd) and forecast (from 24th) data.

In this report, we consider trends in annual and June maxima of three-day temperatures, denoted Tx3x and Tx3x-June for daily maximum temperatures and Tn3x and Tn3x-June for daily minimum temperatures. This definition allows us to analyse the dual impacts of the most acute temperature extremes, and the very warm nighttime temperature lows that affect the ability of people to cool down and recover from high temperatures.

We study the influence of anthropogenic climate change on extreme heat events over this European region by comparing the likelihood and intensity of similar extremes at present with those in a 1.1°C and 0.6°C cooler climate, approximating the climate of 1976 (50 years ago, and the year of one of the most significant heatwaves in the UK in terms of persistently high temperatures), and 2003, when the first major European heatwave of the century occurred.

We also provide analysis of the change in 3-day temperature extremes experienced in European capitals across the study region, accounting for differences in the regional timing and rarity of Tx3x and Tn3x temperature extremes.

2 Observed trends

2.1 Trends in gridded data

At the time of this analysis, the event was still unfolding. There is a strong increase in both 3-day minimum and maximum temperatures (Figures 6-7). The return periods are therefore estimated using a combination of reanalysis, analysis and forecast data available within ERA5 as of 22/06/2026 (the forecast was tested up to 24/06/2026 and found to be stable; Appendix 2.1). The estimated return periods of this event in the present day climate of 2026 depend heavily on whether we assess the likelihood of such an event in June or at some point in the year as a whole. Our analysis suggests that the likelihood of an event to occur at some point during the year in the present climate is about 1 in 25 years for Tx3x and 1 in 20 years for Tn3x. For June only, the analysis suggests that such events are still exceedingly rare in the present day climate, with return periods of approximately 170 years for Tx3x and 240 years for Tn3x. This reflects the difference in sample size of extremes between June and the wider summer period, but primarily the remarkable magnitude of this event in the early summer period.

However, we caution that estimating the likelihood of events in the tail of the distribution or without historical precedent is challenging using the statistical methods used here (i.e. a generalised extreme value distribution with parameters estimated using maximum likelihood; described in section A1.2), as reflected in the high uncertainty ranges (Table 1) (Zeder et al., 2023). This challenge is further compounded by the rapid rate of warming, which is directly linked to an increased likelihood of record-breaking and record-shattering extremes (Fischer et al., 2021; Fischer et al., 2025). We therefore caution that these return periods should not be considered a concrete estimate of present day likelihood and certainly not future occurrence probability for the purposes of planning. Such values could likely be more reliably estimated by incorporating a broader range of drivers and improved statistical techniques (Zhang et al., 2026; Risser et al., 2025). We further note that the choice of return period affects the estimated probability ratios but that the estimated changes in intensity are independent of this. The return periods used for the remainder of this analysis are shown in Table 1. The results for the observational datasets evaluated at these return periods are shown in Table 2.

Event definition		Observed event characteristics (ERA5)		
		Magnitude (C)	Return period (years; 95% C.I.)	Return period used for analysis (years)
Tx3x	June	30.7	166 (30.6, inf)	100
	Annual	30.7	24.8 (10.7, 206)	25
Tn3x	June	18.9	244 (39.5, inf)	100
	Annual	18.9	21.5 (7.81, 207)	20

Table 1: Estimated return periods of Tx3x and Tn3x in both June-only and annually over the study region over western Europe in the combined ERA5 reanalysis, analysis and forecast dataset.

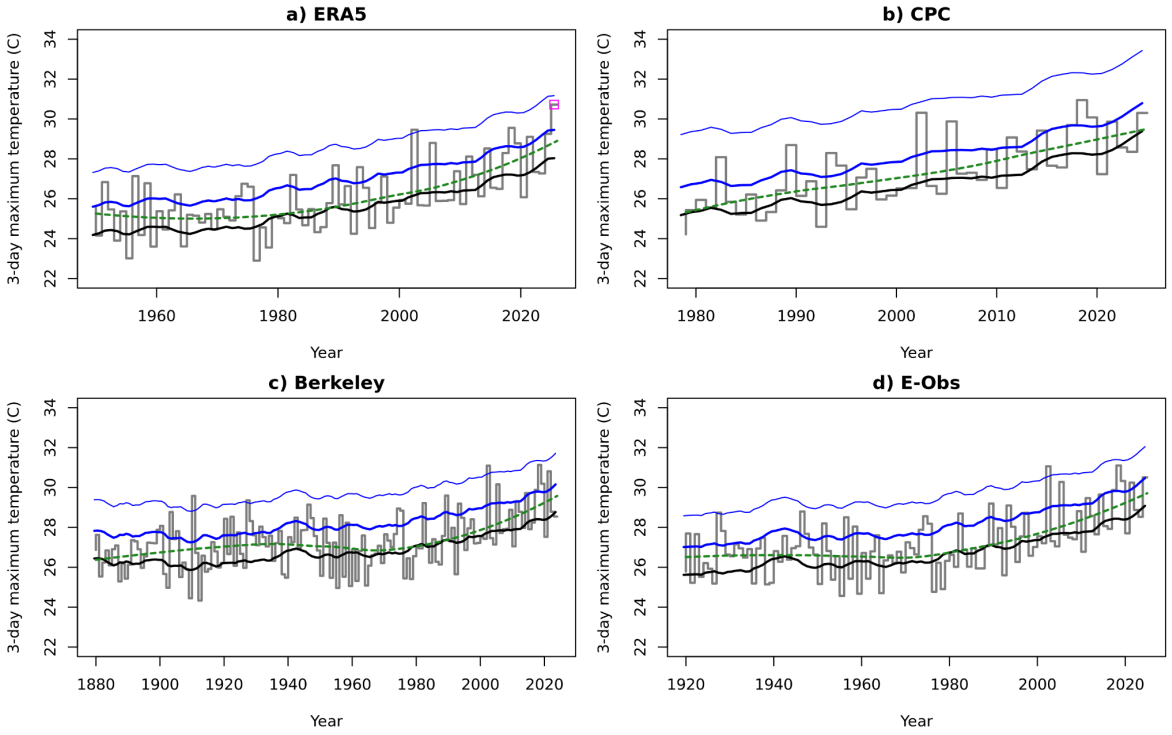

Figure 6: Time series of annual Tx3x in 4 reanalysis and observational datasets for the study region. The event is shown in ERA5 with the pink box. The loess-smoothed trend is shown with the green dashed line and the fitted statistical model that varies with GMST is shown with the black and blue lines, showing the event (black line), and the 1-in-6 (bold blue) and 1-in-40-year (lighter blue) return period event magnitudes.

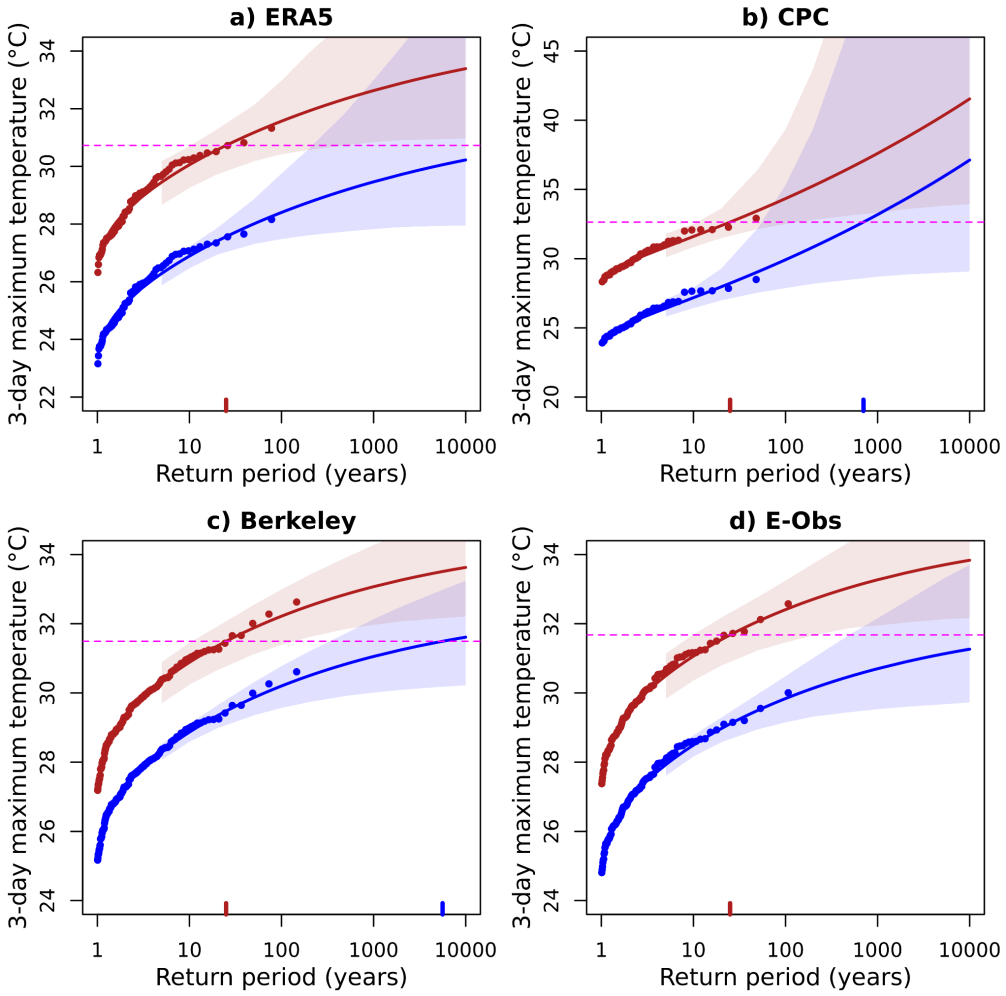

Figure 7: Statistical fits to Tx3x, in a) ERA5, b) CPC, c) Berkeley, and d) E-Obs. The influence of the current GMST is shown with the red vs blue probability curves, showing the present (2026) vs past 1976 warming levels. The magnitude of the 1-in-25-year event is highlighted with a horizontal purple line.

Index	Month(s)	Return period used for analysis	Change since 2003 (~0.6C warming)		Change since 1976 (~1.1C warming)	
			Probability ratio	Change in magnitude (C)	Probability ratio	Change in magnitude (C)
Tx3x	June	100	286 (4.32, >1m)	1.90 (0.93, 3.10)	>1m (11.9, >1m)	3.45 (1.71, 5.69)
	Annual	25	13.9 (2.28, 4980)	1.66 (0.82, 2.84)	580 (3.62, >1m)	3.04 (1.49, 5.21)
Tn3x	June	100	295 (2.88, >1m)	1.31 (0.78, 1.84)	>1m (6.75, >1m)	2.40 (1.42, 3.37)
	Annual	20	163 (4.04, >1m)	0.96 (0.31, 1.66)	>1m (18.3, >1m)	1.75 (0.57, 3.04)

Table 2: Changes in likelihood and intensity in maximum June and Annual 3-day maximum and minimum temperatures, associated with global warming since 2003 (of approximately 0.6°C) and since 1976 (approximately 1.1°C). The results are synthesised across four gridded observational and reanalysis datasets.

The results are clear across all datasets and for all indices; the June 2026 heatwave in Europe has become much more likely and intense as a result of human-induced climate change. Fifty years ago in 1976, when the world was approximately 1.1°C cooler, such a warm and widespread heat event would have been virtually impossible, whether we consider an event occurring only in June or at any point during the year. Whilst, the 1976 heatwave saw temperatures reach nearly as high as this event at the UK peak location, this event was strongest further south and had a much larger spatial extent. Equivalently, a heat event of a similar estimated rarity has become much hotter. The 3-day maximum temperatures have become more than 3 degrees hotter, and the 3-day minimum temperatures about 2 degrees hotter (Table 2). Since 2003, with warming of approximately 0.6°C, such events have become tens to hundreds of times more likely. The 3-day maximum temperatures have warmed by 1.5-2°C and the 3-day minimum temperatures by around 1°C.

Two points of note emerge from this analysis. First, heat extremes in June in the study area are increasing at a faster rate than the overall annual change, at a ratio of approximately 1.1-1.2 for Tx3x and around 1.4 for Tn3x. Further, June is found to be the fastest warming month of the year in the study region (Fig. A3.2). This suggests that earlier summer heat is increasing most rapidly. Second, maximum temperatures are increasing faster than daily minimum temperatures, though both are increasing at a rate vastly above the average global warming, with maximum temperatures increasing at around triple the global warming rate and minima by around double. To summarise, heat extremes are becoming much more likely and intense across living and even recent memory.

2.1.1 Influence of modes of natural variability

The El-Niño Southern Oscillation (ENSO) and North Atlantic Oscillation (NAO) are both possible drivers of summer conditions in Europe. Therefore, we first investigate the effect of including these as additional covariates in the statistical model (section A1.2). ENSO is represented by the relative Niño3.4 index, averaged over multiple periods to test both the peak of the natural oscillation and lagged effects from this: December-February, March-May and June-August (excluding 2026 for the latter). The NAO was assessed using the June-August mean and with data up to 2023. However, fitting a statistical model using both GMST and these indices as covariates to the annual Tx3x does not improve the compromise between fit and model complexity, according to the AIC, than GMST alone (Table 3). This holds for all datasets. This suggests that these indices do not play a major role in this extreme and are therefore not considered for the remainder of this study.

Dataset	AIC scores				
	GMST only	NAO (JJA)	ENSO (DJF)	ENSO (MAM)	ENSO (JJA)
ERA5	**236.28**	236.88	237.58	238.00	238.28
CPC	**143.77**	145.73	144.79	145.74	145.69

Berkeley	**329.41**	330.63	331.19	331.26	331.01
E-Obs	**449.73**	451.23	451.69	450.98	451.39

Table 3: AIC scores for statistical models fitted to Tx3x calculated from each observational and reanalysis dataset used in this analysis. The lowest score indicates the best compromise between goodness-of-fit and model complexity and is highlighted in **bold text**.

2.2 Regional trends

The effect of human-caused global warming on peak summer temperatures is clear across Europe, but the rate of warming and the extremeness of the current heatwave vary across the continent. Figure 8 shows the results of fitting a nonstationary GEV, in which local Tx3x (top row) and Tn3x (bottom row) shift linearly with GMST, to each grid cell in the study region in the ERA5 dataset (the only dataset for which a forecast of the continued heatwave progression was available). Panel a shows the 3-day maximum temperatures reached in each grid cell in 2026; while these did not necessarily occur on the same day in each cell, across almost the whole region the peak occurred between June 22nd and June 29th (see Appendix, Figure A3.1). Panel b in each row shows how unusual these temperatures are locally. The peak daytime temperatures would be unusual at any time of the year across much of the study region, with return periods of more than 10 years, and in some regions very extreme, with return periods of more than 100 years in western France and across much of eastern Europe. Panel c shows the local warming since 2003, when the world was around 0.6°C cooler than in 2026. Western Europe has warmed most rapidly, with peak daytime temperatures up to 4°C hotter than they would have been 23 years ago in southern England, as well as much of France, Belgium and the Netherlands. Similarly, as indicated in panel d, extreme daily maximum temperatures are now more than 10 times more likely to occur across most of Europe since 2003, with the most extreme temperatures in western France and northern Germany now more than 100 times more likely due to human-caused warming.

Nighttime temperatures were even more unusual across much of southern England and throughout western, central and eastern Europe (bottom row, panels a & b). Locally, nighttime temperatures have warmed slightly less than daytime temperatures, but still substantially more than for the planet as a whole (panel c). The likelihood of experiencing such warm nighttime temperatures has increased by more than tenfold since 2003 across much of Europe, and by more than 1000-fold in the most extreme cases (panel d).

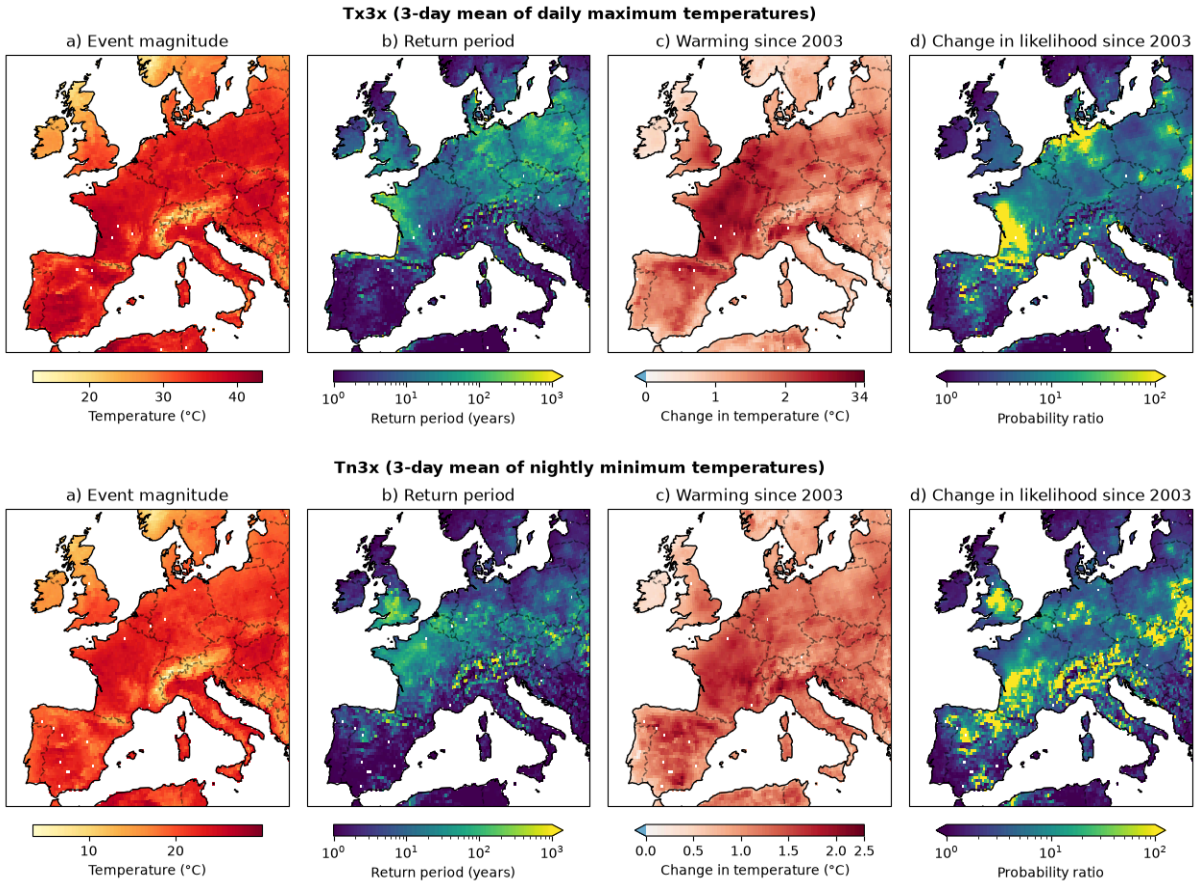

Figure 8: upper, Tx3x (annual maximum 3-day mean of daily maximum temperatures) and lower, Tn3x (annual maximum 3-day mean of daily minimum temperatures). From left to right, maximum three-day temperatures for all locations in the study region; return period in 2026 (expected number of years between events of this intensity); change in intensity due to climate change since 2003 (°C); probability ratio (change in likelihood) of the likelihood of the heat event in 2026 compared to in 2003, when the world was around 0.6°C cooler. All data: ERA5.

While Figure 8 shows that the temperatures experienced during this heatwave would be considered extreme at any time of year, they are even more unusual in June. Table 4 lists the peak 3-day daytime and nighttime temperatures reached in each of the capital cities within the study region, along with the return period according to ERA5, which indicates how rare such temperatures are in June as well as for any time of the year. In 18 of the 19 cities, the hottest three-day period is the hottest on record for June (marked with a single asterisk), and in nine of those, also the hottest on record at any time of year (marked with a double asterisk). In many capitals, the temperatures were unusually high for June, with return periods well in excess of 100 years in ten of the capitals - although, as noted above, the exact numbers are highly uncertain due to the extremeness of the temperatures reached. Nonetheless, similar temperatures are not unusual during the peak of summer in today's climate, with much lower annual return periods. For capital cities in southern Europe (Zagreb, Rome and Madrid) similar June daytime temperatures are becoming relatively typical in today's climate, despite being the hottest 3-day June temperatures in the ERA5 record, illustrating how rapidly the climate is changing.

Similarly, in 16 of the 19 capitals within the study region the hottest three nights were the hottest on record for June, and in ten of those, also the hottest on record for any time of year. Again, the temperatures are very extreme for June, with twelve of the capitals having return periods well above

100 years; in London, Paris, Luxembourg, Brussels and Budapest, similarly high nighttime temperatures would be extremely unusual at any time of the year, highlighting the extreme intensity of this event.

	Tx3x			Tn3x		
	Magnitude (°C)	Return period		Magnitude (°C)	Return period	
		June	Annual		June	Annual
Oslo	25.84	4.36 (2.11, 11.6)	1.66 (1.23, 2.42)	15.88	8.32 (4.3, 29)	1.33 (1.1, 2.09)
Stockholm	28.07*	84.2 (19.3, Inf)	4.84 (2.9, 11.2)	18.45*	38 (12.3, 2700)	2 (1.37, 3.55)
Copenhagen	29.27*	37.5 (7.69, Inf)	3.88 (1.9, 8.53)	19.4*	161 (43.8, Inf)	5.29 (2.77, 15.5)
London	32.73**	65.5 (21.5, Inf)	11.2 (5.45, 35.6)	21.07**	331 (64.9, Inf)	138 (26.8, Inf)
Dublin	25.37*	145 (32.9, Inf)	14.1 (5.43, 46.9)	15.76	9.8 (5.37, 48.7)	2.06 (1.37, 3.43)
Paris	38.08**	188 (44.9, Inf)	19.4 (7.26, 78.1)	25.57**	213 (48.1, > 1m)	247 (55, Inf)
Brussels	35.81**	192 (37.7, Inf)	17.3 (7.07, 103)	23.71**	1130 (103, Inf)	165 (45.4, Inf)
Amsterdam	32.21*	119 (24.9, Inf)	6.86 (3.13, 55.3)	20.85*	238 (36.8, Inf)	9.48 (3.87, 31.1)
Luxembourg	36.36**	319 (49.5, Inf)	24 (10.7, 103)	23.07**	250 (54.9, Inf)	53.8 (21.4, 723)
Bern	34.08*	58.5 (19, 4590)	9.41 (4.39, 28.3)	20.83**	368 (59.1, Inf)	16.7 (8.15, 93.1)
Berlin	38.23**	683 (74.8, Inf)	41.2 (14.3, 328)	22.99**	242 (37, Inf)	14.6 (5.42, 69.3)
Vienna	38.35**	516 (66.9, Inf)	34 (14.2, Inf)	24.52**	394 (62.5, Inf)	38.5 (15, 12700)
Prague	37.47**	484 (65.4, Inf)	36.2 (16.6, 197)	21.85**	318 (52.6, Inf)	15.1 (7.21, 43.2)
Bratislava	38.08**	440 (52.6, Inf)	24.3 (11.1, 439)	24.38**	374 (54.3, Inf)	25.2 (8.97, 152)
Budapest	38.74**	253 (47.6, Inf)	25.1 (10.9, 157)	26.08**	453 (74.2, Inf)	76.5 (21.5, 240000)
Zagreb	35.55*	6 (3.03, 16.9)	2.08 (1.41, 3.28)	23.53*	96.2 (19, Inf)	5.09 (2.51, 12.9)
Ljubljana	34.51*	36.8 (12.4, 1190)	6.04 (3.34, 14.1)	19.91*	19.7 (6.75, 749)	2.19 (1.48, 4.33)
Rome	36.63*	19.2 (7.4, Inf)	4.73 (2.64, 16.6)	23.47*	12.7 (5.6, 54.3)	1.92 (1.4, 3.92)
Madrid	39.03*	7.14 (3.44, 21.2)	2.56 (1.75, 4.99)	23.1	6.32 (3.26, 31)	1.61 (1.26, 2.52)

Table 4: Tx3x/Tn3x and return period of the event in the context of both June heatwaves and of heatwaves occurring at any time of year, according to reanalysis, analysis and forecast data. Single asterisk indicates the hottest June temperatures since 1950; double asterisk indicates the hottest annual temperatures since 1950. Darkest shading highlights return periods greater than 100; medium shading highlights locations with return periods of 50-100 years; lightest shading highlights locations with return periods of 20-50 years. Numbers in parentheses give 95% confidence intervals. All data from ERA5.

Table 5 shows the estimated change in Tx3x and Tn3x in the 19 capitals since 2003, when the world was around 0.6°C cooler, both for June and for occurrences at any time of year. These trends are estimated in four gridded data products (ERA5, E-Obs, CPC and Berkeley Earth; see Section A1.1) and averaged to obtain a robust estimate of observed warming. In 15 of the capitals, peak June daytime temperatures have warmed more than twice as much as the planet as a whole. In 12 of the capitals, June Tx3x temperatures have warmed by more than 0.2°C more (indicating more than simple rounding errors) than the annual 3-day daytime maxima. In 13 of the capitals, the warmest June 3-day nighttime temperatures have warmed more than twice as much as the planet as a whole, and in 15 capitals, the warmest June nights have warmed more than the warmest nights overall. In almost all

cities outside of Scandinavia, daily 3-day averaged maximum temperatures are warming more than 3-day averaged nighttime temperatures.

	Tx3x (daily maximum)		Tn3x (nightly minimum)	
	June	**Annual**	**June**	**Annual**
Oslo	0.5 (-0.7, 1.8)	0.5 (-0.7, 1.8)	0.5 (-0.5, 1.5)	0.4 (-1.3, 2)
Stockholm	0.7 (-0.2, 1.9)	0.5 (-0.9, 2.1)	0.9 (0.2, 1.6)	0.6 (-0.7, 1.9)
Copenhagen	0.7 (-0.4, 1.9)	0.7 (-0.3, 1.8)	0.7 (-0.2, 1.6)	0.6 (-0.5, 1.8)
London	1.7 (0.7, 2.8)*	2.1 (1.2, 3.1)*	1 (0.5, 1.6)	0.9 (0.3, 1.5)
Dublin	1.1 (-0.1, 2.2)	0.9 (-0.1, 1.9)	1 (0.3, 1.8)	0.6 (-0.1, 1.2)
Paris	2.4 (0.8, 4.1)*	2.4 (1.1, 3.7)*	1.7 (1.1, 2.2)*	1.3 (0.7, 2)*
Brussels	1.9 (0.8, 3.1)*	2 (0.9, 3.3)*	1.3 (0.6, 2.1)*	1 (0, 2.1)
Amsterdam	1.7 (0.6, 2.8)*	1.9 (0.7, 3.2)*	1.3 (0.7, 2)*	0.9 (0.2, 1.8)
Luxembourg	2.4 (0.8, 4)*	2 (0.9, 3.2)*	1.4 (0.6, 2.3)*	1.1 (0.1, 2.1)
Bern	2.1 (0.5, 3.8)*	1.7 (0.4, 2.9)*	1.8 (0.6, 3)*	1.1 (0.2, 2.1)
Berlin	1.7 (0.4, 3.1)*	1.4 (0.1, 2.9)*	1.2 (0.6, 2)	1 (0.1, 1.9)
Vienna	2.4 (1.4, 3.5)*	1.7 (1, 2.5)*	1.7 (0.8, 2.7)*	1.3 (0.7, 2.1)*
Prague	1.9 (0.9, 3)*	1.6 (0.7, 2.5)*	1.3 (0.6, 2)*	0.9 (-0.3, 2.1)
Bratislava	1.9 (1, 3)*	1.4 (0.6, 2.2)*	1.6 (1.1, 2.3)*	1.2 (0.5, 2)
Budapest	1.8 (0.5, 3.1)*	1.2 (0.2, 2.1)	1.5 (0.5, 2.5)*	1.2 (-0.1, 2.6)
Zagreb	2.2 (1.2, 3.3)*	1.3 (0.3, 2.5)*	1.8 (0.8, 2.8)*	1.3 (0.4, 2.1)*
Ljubljana	2.5 (0.9, 4.1)*	1.7 (0.8, 2.7)*	1.8 (0.8, 2.9)*	1.3 (0.5, 2.1)*
Rome	2.7 (0.9, 4.5)*	1.7 (0.6, 2.8)*	1.6 (0.1, 3.2)*	0.8 (-0.6, 2.3)
Madrid	2.3 (1.5, 3.1)*	1.6 (0.9, 2.1)*	2 (0.8, 3.2)*	1.4 (0.5, 2.4)*

Table 5: Increase in 3-day extreme temperatures in each capital since 2003, when the world was 0.6°C cooler. Single asterisk and shading indicates estimated warming of more than double the global mean. Numbers in parentheses give 95% confidence intervals. Synthesised estimate from four observational data products (see Appendix A1.1 for details).

2.3 Circulation analogues

Figure 9a shows the event day, characterized by a pronounced ridge (positive Z500 anomaly) extending across the Mediterranean and southern Europe, accompanied by a deep trough (negative Z500 anomaly) over the North Atlantic and northern Europe. This circulation pattern promotes the advection of warm air from North Africa into western Europe, resulting in elevated temperatures across the region. Composite patterns for the historical (1950–1979) and present-day (1994–2023) periods are shown in Figures 9b and 9c, respectively, and reveal a remarkably similar large-scale circulation structure. The differences between the two periods are small (generally within ±20 m) and are not statistically significant over the majority of the region (Figure 9d), indicating that intensity of the large-scale atmospheric circulation associated with these events has remained largely unchanged. However, the frequency of occurrence of this circulation type has increased since 1950, although this increase is not statistically significant (Figure 10). An increasing trend toward more frequent southerly flows explains up to 0.8°C per degree of global warming in Western European heat extremes (Vautard et al., 2023).

Figure 9e–h shows the maximum temperature (Tmax) associated with the event and its historical and present-day analogues. The event was characterized by exceptionally warm conditions across western, central, and southern Europe, with maximum temperatures exceeding 30°C over large areas. Comparison of the climatological composites indicates that present-day temperatures (1994–2023) are statistically significant and higher than those associated with the same circulation pattern during 1950–1979. The strongest warming is observed over France, Germany, central Europe, and parts of the Balkans and eastern Europe. In many regions, maximum temperatures are approximately 1–4°C higher under a comparable large-scale atmospheric configuration, highlighting the influence of background climate warming on the intensity of heat extremes.

Figures 9i–l show the minimum temperature (Tmin) associated with the event and its historical and present-day analogues. Nighttime temperatures are also consistently higher in the present-day climate compared to the 1950–1979 period, with a widespread warming signal evident across most of Europe. Under a similar large-scale circulation pattern, minimum temperatures are generally 1–3°C higher, with some regions experiencing increases approaching 4°C.

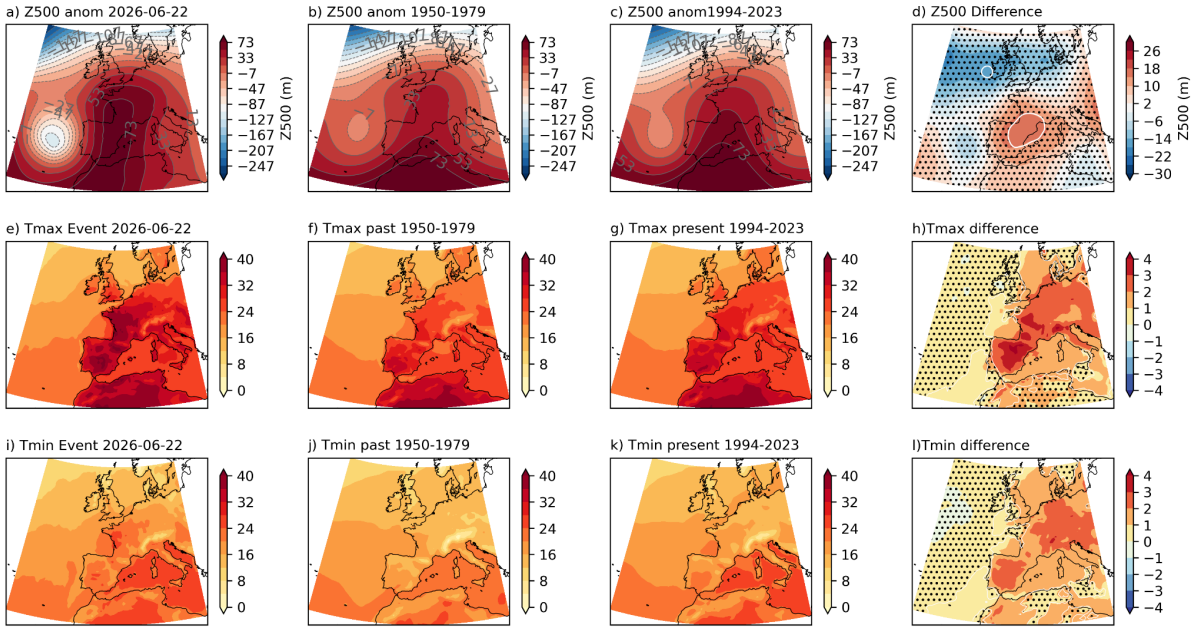

Figure 9. C*hanges in atmospheric analogues. (a) 500hPa geopotential height field (m) for the event, 22 June 2026. b) Composite of the top 28 analogue days from the past period, 1950-1979. c) Composite of the top 28 analogue days from the present period, 1994-2023. d) Difference between the composites of past and present (present minus past). e-h) as in a-d for the daily maximum temperature field (°C). i-l) as in a-d for the daily minimum temperature field (°C). Z500 used to identify analogues in all plots. Dots signify regions where the signal is not significant based on a two-sided t-test.*

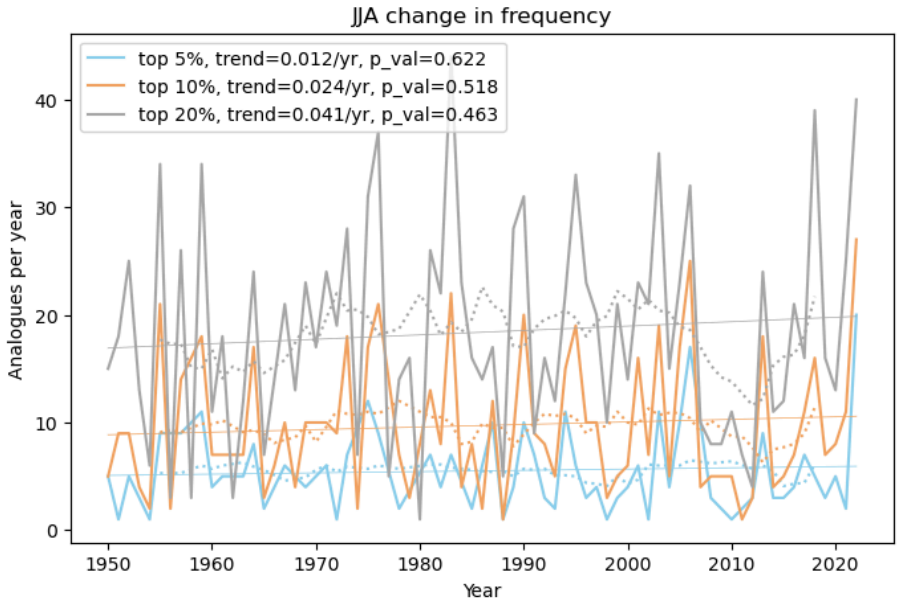

Figure 10. *Trends in frequency of the most similar events. Number of "good" analogues per year (in JJA) at three threshold levels: the closest 5%, 10% and 20% of most similar days (based on Euclidean distance of Z500 field over the region [25°E to 20°W, 40° to 60°N]. Linear trend lines (solid thin lines) and multiannual trends (dotted lines) are plotted, with trend per year and p-value shown.*

2.4 Summary of observed trends

Based on temperatures averaged over the full study region, June heat of this magnitude has an estimated return period exceeding 100 years. When assessed on an annual basis, it represents about a 25-year event for Tx3x and approximately a 20-year event for Tn3x. Due to the increasing rapidity of climate change, the estimates of these event rarities are conservative (Zeder et al., 2023). Across Tx3x/Tn3x and June/annual event definitions, we find that this event was near impossible in the climate of 50 years ago and exhibits an increase in likelihood of ~300x since 2003 for either minimum or maximum temperatures occurring in June. Annually, we found a 160x increase in the chance of Tn3x condition occurring at any time in the summer since 2003, and a 14x increase in the chance of Tx3x.

These overall numbers are for the contemporaneous heat throughout the entire study region; however, in reality, the heatwave moved from west to east, with the locus initially in western France moving across northern and central Europe. Figure 8 shows the gridded event magnitude for annual Tx3x and Tn3x, the rarity of this magnitude in 2026, and the change in intensity and likelihood of this event relative to a 2003 climate.

Many media reports cited the "heat dome" that contributed to this heat event (Clun, 2026; Ghaffar, 2026; ITV, 2026). Such circulation conditions are characteristic of most major European heatwaves, and we tested whether there is a changing frequency of similar southerly flow events due to climate change, in accordance with evidence of such changes in the literature (Vautard et al., 2023). An increase in frequency was observed, but the linear regression of this trend was not found to meet a statistical significance level of $p<0.05$. The June 2025 heatwave occurred under a southerly flow circulation pattern broadly similar to historical analogues. However, a similar circulation pattern now

produces significantly hotter temperatures than it did in the mid-20th century because the climate baseline has warmed.

3 Vulnerability and exposure

Risk is determined not only by the hazard itself (the heatwave in this case), but also by the interaction between hazard, exposure, vulnerability, and coping capacity (Reisinger et al., 2020). Across Europe, rising temperatures, combined with a large urban population, ageing populations, and persistent adaptation gaps are increasing the risk of devastating impacts despite progress in warning systems and heat action planning (World Bank, 2024).

Exposure is particularly concentrated in **urban areas,** where large populations, critical infrastructure, and economic activity coincide with urban heat island (UHI) effects. Major cities can experience substantially higher temperatures than surrounding rural areas, especially in densely built neighborhoods with limited vegetation and surface water (Chakraborty et al., 2019; Marando et al., 2022). Heat exposure can also vary significantly between neighborhoods due to differences in housing, green space, working conditions, with cities such as Copenhagen, Berlin, London, and Paris concentrating UHI in lower-income neighborhoods (Chakraborty et al., 2019). Across Europe, urban heat exposure is further amplified by extensive building and infrastructure which were constructed before modern thermal building standards and not designed for prolonged extreme heat (EEA, 2023). The current event demonstrates how exposure is shaped not only by outdoor temperatures but also by the **thermal performance of buildings** and enclosed environments. In France, fatalities have been linked to overheating inside vehicles and indoors, illustrating how prolonged heat can become life-threatening when housing and other built environments aggravate the heat (Kar-Gupta & Young, 2026; Peseckyte, 2026a). This is also relevant in the UK, Ireland, Benelux, Germany, Scandinavia, and parts of Central Europe where buildings were historically optimized to retain heat rather than dissipate it (Brimicombe et al., 2021; Kapur et al., 2024). The disruption of education services during the current heatwave, including school closures and reduced schedules across thousands of educational facilities in France and the UK, further demonstrates how many public buildings and institutions remain insufficiently adapted to extreme temperatures, worsening risks for students and staff (BBC, 2026a; Bland, 2026; Gulf News, 2026).

Vulnerability to the heat is further shaped by **demographic and health factors**. Older adults, people with chronic cardiovascular, diabetes, respiratory, and renal conditions, socially isolated individuals, residents of care facilities, houseless populations and people living in poor-quality housing face elevated risks of heat-related illness and mortality (Åström et al., 2015; Bouchama et al., 2017; Schwarz et al., 2021; Colucci et al., 2021). The ongoing heatwave has already placed significant pressure on healthcare systems, with hospitals reporting increases in admissions for heat-related illnesses including dehydration and cardiovascular stress (Peseckyte, 2026b). In France's Landes department, emergency services recorded a 20% increase in calls on 21 June (TTW, 2026). Further, extreme heat can impact sleep and mental health (WHO, 2026).

This is also the high season for tourism in Europe. An often overlooked group of people is tourists, who may not be acclimatized and may also have underlying health conditions, making it harder to cope in the heat. The large number of drowning fatalities recorded during the current event, including at least 40 in France and five in Germany, also highlights how behavioral responses to heat, like

seeking relief in rivers, lakes, and other water bodies, can create additional risks (Kar-Gupta & Young, 2026; Joubioux, 2026; France24, 2026). **Population ageing** is a key driver of increasing heat vulnerability across Europe, with roughly one in five people already older than 65 years, and the oldest-age groups are expected to grow steeply over coming decades (Eurostat, 2026). A growing body of literature highlights impacts of extreme heat on pregnancy and pregnant women (Grimshaw et al, 2026). More attention must be paid to **gendered impacts** and how these impacts will further increase inequity. Moreover, vulnerable groups such as unhoused populations, and people living in prisons may have no access to cooling or any other option to cope in current heat conditions. Despite advances in heat action planning, many of the housing related heat risks are deep rooted and historical. For example, many migrants who live in poorer neighbourhoods may not have the means to retrofit their houses or afford to pay rent in houses that have cooling (Anguelovski et al, 2024). **Outdoor workers** are at a higher risk of heat exposure due to their livelihoods. Agricultural workers, and particularly undocumented migrants working as farm labour for example are at an elevated risk of exposure. This exposure comes with lack of social protection or occupational safety frameworks (EEA, 2025).

Heat risk also affects important **ecosystems and critical infrastructure**. In the Mediterranean region, drought and water stress often compounds extreme heat, increasing risks to agriculture, ecosystems, and water supply (Zachariah et al., 2022). There is elevated danger of fires in forests (Joint Research Center, 2026) and warnings have been issued for wildfires, which could have devastating impacts. In France's Cher department, a wildfire burned at least 25 hectares of crops and prompted the evacuation of approximately 50 people (Symons, 2026). Research highlights that European forests are at risk of high damage and experience reduced forest cover already due to a combination of droughts and extreme temperatures (Knutzen et al, 2025). Extreme heat is also affecting ecosystems more broadly. In Belgium, wildlife rescue centres reported a surge in heat-stressed animals, particularly young birds, highlighting the sensitivity of ecological systems to periods of exceptionally high temperatures (Reuters, 2026).

Further, there is increased need and demand for electricity supply. While air conditioning (AC) remains relatively uncommon in Europe, with ownership rates of around 20% (Voswinkel et al., 2025), adoption is increasing rapidly, especially during heatwaves. The lack of AC increases exposure to heat, but rapid growth in cooling demand is also creating new pressures on Europe's electricity systems, and, if supplied by carbon-intensive energy sources, may contribute to further climate change. Beyond unadapted housing for the present climate, socioeconomic inequities also exacerbate risk due to reduced access to adaptation resources. At the same time, heat can directly constrain energy production. Elevated temperatures in France's Rhone and Garonne rivers have resulted in restrictions on electricity generation at nuclear power stations including Saint-Alban and Blayais, with knock-on energy price spikes (Straits Times, 2026; France24, 2026). As climate change makes heatwaves hotter, longer, and more frequent, summer energy poverty is emerging as a growing concern, with many households unable to afford the cooling needed to maintain safe indoor temperatures (European Commission, n.d.). Additional disruptions have included power outages affecting approximately 68,000 households in Brittany and the cancellation of at least 71 intercity train services across France due to concerns over damage to overhead power lines and rail infrastructure. Across the UK, rail operators have also imposed speed restrictions and advised against travel due to risks of track buckling under extreme temperatures (BBC, 2026c; Reuters, 2026;

Niranjan, 2026). These have major implications for healthcare, tourism, agriculture and other related sectors.

Heat risk governance varies across the region. Following the 2003 European heatwave, many countries - including France, Spain, Portugal, Italy, Germany, and the UK - implemented early warning systems, heat-health action plans, and preparedness measures that have contributed to reductions in heat-related mortality and strengthened institutional response capacity (Martinez-Solanas & Basagana, 2019; Sanchez Martinez et al., 2022). However, the current event illustrates that even where preparedness measures exist, coping capacity can still be stretched during severe heat events. In the UK, East Surrey Hospital declared a critical incident due to exceptional demand, restricting services to life-threatening emergencies and redirecting non-urgent patients elsewhere (Peseckyte, 2026b).

Today, most European countries have a heat warning system in place, while heat-health action plans have become increasingly widespread at both national and sub-national levels (EEA, 2025). Many countries, including France, UK, Germany, Italy, and Spain have issued highest-level heat warnings (Badshah et al., 2026). A study found that such plans reduced heat-related mortality by approximately 25% across 14 European countries since 1990, preventing over 14,000 deaths (Urban et al., 2025). However, many warning systems remain primarily hazard-focused, with limited integration of real-time health surveillance and epidemiological forecasting (Roye et al., 2026). Large differences persist in heat-health surveillance, mortality estimation, and warning methodologies across Europe, despite the availability of relatively robust health and meteorological data. Furthermore, urban greening, improved building design including the integration of passive cooling measures, building retrofitting, targeted outreach to vulnerable populations, and strong social networks can further reduce heat risk (Burkart et al., 2016; Marando et al., 2022; Klinenberg, 2015). However, implementation remains uneven across countries, regions, and municipalities, leaving significant residual risk despite progress.

Heatwave related deaths are avoidable. Overall, the 2026 June heatwave gives us a glaring reality of improving heat risk governance and implementing heat action plans. Extreme heat impacts cuts across various sectors. However, impacts are felt more severely by some of the most marginalised and vulnerable groups. Addressing deep rooted questions of vulnerability and access to resources and social protection must be central to future heat risk governance mechanisms across different countries.

Data availability

All time series used in the attribution analysis are available via the Climate Explorer.

Acknowledgements

This work used Imperial College Research Computing Service, DOI: 10.14469/hpc/2232.

This work used the KNMI Climate explorer web tool (https://climexp.knmi.nl/start.cgi).

References

All references are given as hyperlinks in the text.

Appendices

A1 Data and methods

A1.1 Observational data

We first use observational and reanalysis data to estimate the return period of a similar event in the present day and to assess the historical trends with increasing GMST. The datasets used are as follows:

- **ERA5** - The European Centre for Medium-Range Weather Forecasts's 5th generation reanalysis product, ERA5, is a gridded dataset that combines historical observations into global estimates using advanced modelling and data assimilation systems (Hersbach et al., 2020). We use VARIABLE data from this product at a resolution of 0.25°×0.25°, from the years 1950 to present. Reanalysis is available until the end of May 2026, and extended with analysis data from June 1st-23rd and forecast data from June 24th-30th. Changes in the forecast data were tracked prior to release of this report, with peak temperatures found to be relatively stable in successive forecasts (see Appendix A2).
- **E-OBS** - This is a gridded land-only observation dataset of Europe, formed from the interpolation of station-derived meteorological observations (Cornes et al., 2018). We use version 32.0e of this dataset, at spatial resolution 0.25° × 0.25° gridded daily maximum and minimum temperatures, from 1920-present.
- **CPC -** This is the gridded product from NOAA PSL, Boulder, Colorado, USA known as the CPC Global Unified Daily Gridded data, available at 0.5° x 0.5° resolution, for the period 1979-present. We use daily maximum and minimum temperatures. Data are available from NOAA.
- **Berkeley -** Berkeley Earth land and ocean gridded temperature data (Rohde & Hausfather, 2020). Global datasets begin in 1850, with some land-only areas reported back to 1750. We use daily maximum temperature from 1897 to 2024 at 1° x 1° resolution, available from the Berkeley Earth website.

As a measure of anthropogenic climate change we use the (low-pass filtered) global mean surface temperature (GMST), where GMST is taken from the National Aeronautics and Space Administration (NASA) Goddard Institute for Space Science (GISS) surface temperature analysis (GISTEMP, Hansen et al., 2010 and Lenssen et al. 2019). To remove the effect of the El Niño - Southern Oscillation on global mean temperatures, we use a four-year running mean of the GMST, centred on the third year.

As a measure of the El Niño - Southern Oscillation cycle (ENSO) we use the detrended Niño3.4 index. This is computed from NOAA's ERSST v.5 sea surface temperatures, by subtracting the mean tropical SST (20S-20N) from the mean SST over the Nino3.4 region (5S-5N, 170W-120W). This

index is therefore adjusted to remove the linear trend associated with climate change as proposed in van Oldenborgh et al., 2021, but without rescaling each calendar month.

As a measure of the North Atlantic Oscillation (NAO) we use the June-August mean of the normalized pressure difference between Gibraltar and SW Iceland (Reykjavik) (Jones et al., 1998), with monthly index calculated by the Climate Research Unit and available here.

A1.2 Statistical methods

Methods for observational and model analysis and for model evaluation and synthesis are used according to the World Weather Attribution Protocol, described in Philip et al., (2020), with supporting details found in van Oldenborgh et al., (2021), Ciavarella et al., (2021), Otto et al., (2024) and here. The key steps used here are: (3) trend estimation from observations and (6) synthesis of the attribution statement.

In this report we analyse time series of June- and annual-maxima of 3-day daily maximum and minimum temperatures over the study region, which is land areas bounded by 40-60N, -10.5-20E. A nonstationary GEV distribution is used to model these variables. The distribution is assumed to shift linearly with the covariates, while the variance remains constant. For each time series we calculate the return period and intensity of the event under study for the 2026 GMST and for 1.1°C and 0.6°C cooler GMST: this allows us to compare the climate of now and of the past periods (based on the Forster et al., 2026), by calculating the probability ratio (PR; the factor-change in the event's probability) and change in intensity of the event.

In order to examine the effect of the ENSO and NAO phase on Tx3x and Tn3x alongside that of increasing GMST, we extend the nonstationary model to accommodate an additional covariate. The variable of interest, X, is assumed to follow a GEV distribution in which the location parameter varies with both GMST and ENSO or NAO:

$$X \sim GEV(\mu, \sigma, \xi \mid \mu_0, \sigma_0, \alpha, \beta, T, I),$$

where X denotes the variable of interest, 3-day maximum or minimum temperatures; T is the smoothed GMST; I is the detrended Niño3.4 index or NAO index; μ_0, σ_0 and ξ are the location, scale and shape parameters of the nonstationary distribution; and α, β are the trends due to GMST and ENSO or NAO, respectively. As a result, the location and scale of the distribution have a different value in each year, determined by both the GMST and Niño3.4 or NAO states. Maximum likelihood estimation is used to estimate the model parameters, with

$$\mu = \mu_0 + \alpha T + \beta I \qquad \text{and} \qquad \sigma = \sigma_0.$$

A1.3 Circulation Analogues

Atmospheric flow analogues can be used to assess changes in the intensity of dynamically similar events or changes in the frequency of occurrence of particular circulation patterns (Vautard et al., 2023; Jézéquel et al., 2018, Thompson et al 2024). Here we use ERA5 data to assess analogues

identified from 500 hPa geopotential height (Z500) since 1950, to detect changes in the frequency of circulation patterns similar to those associated with the heatwave.

To identify the most similar events, we compute the Euclidean distance between the Z500 anomaly field of 22 June 2026 and every other day (1950–2024) over the region bounded by [25°E to 20°W, 40° to 60°N] for the season of June-August (JJA). To avoid double-counting persistent events, the identified events must be separated by at least 5 days. The region and circulation variables were determined by assessing the event itself and earlier current understanding of the circulation drivers of similar events (Holgate et al 2023).

To detect trends in the circulation pattern and intensity since 1950 we identify the closest 28 analogues across the two periods (1950-1979 and 1994-2023). This corresponds to the closest 1% of days in each period. The average weather conditions associated with the two sets of analogues - called 'composites' - are then compared to assess differences between the two periods. We also assess the change in frequency of the closest analogues through time. This is assessed at three different thresholds - the upper 5% of days, upper 10%, and upper 20%. Differences in modes of internal variability between the two time periods can also induce differences in the weather conditions, therefore we cannot identify the role of climate change solely by comparing analogue sets in reanalyses.

A2. Stability of temperature forecasts

To check that the forecasted temperatures are stable, we tracked the development of the forecasts over successive days during the preparation of the report (Figure A2.1). While expected temperatures from June 29th onwards were somewhat lower in the latest available forecast (green line), 3-day averaged temperatures leading up to and including the peak of the heatwave remained stable (Table A2.1). We are therefore confident that the timing and magnitude of the event are well forecasted and that the results of our analysis would not be substantively different if repeated using analysis or reanalysis data.

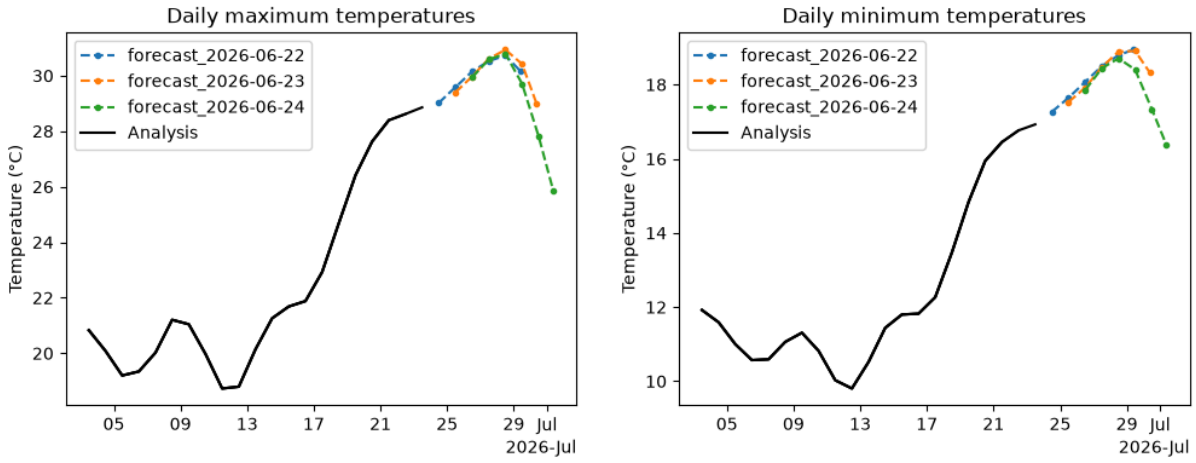

Figure A2.1: 3-day running mean of daily maximum and minimum temperatures in ERA5 analysis (solid black line) and successive forecasts (dashed coloured lines), averaged over the study region (10.5°W to 20°E, 40 to 60°N).

	Tx3x		Tn3x	
Forecast date	**Magnitude 30.7**	**Date**	**Magnitude**	**Date**
June 22nd	30.72	June 28th	18.94	June 29th
June 23rd	30.93	June 28th	18.89	June 28th
June 24th	30.78	June 28th	18.71	June 28th

Table A2.1: Magnitude and timing of peak Tx3x and Tn3x in successive ERA5 forecasts.

A3. Supplementary figures

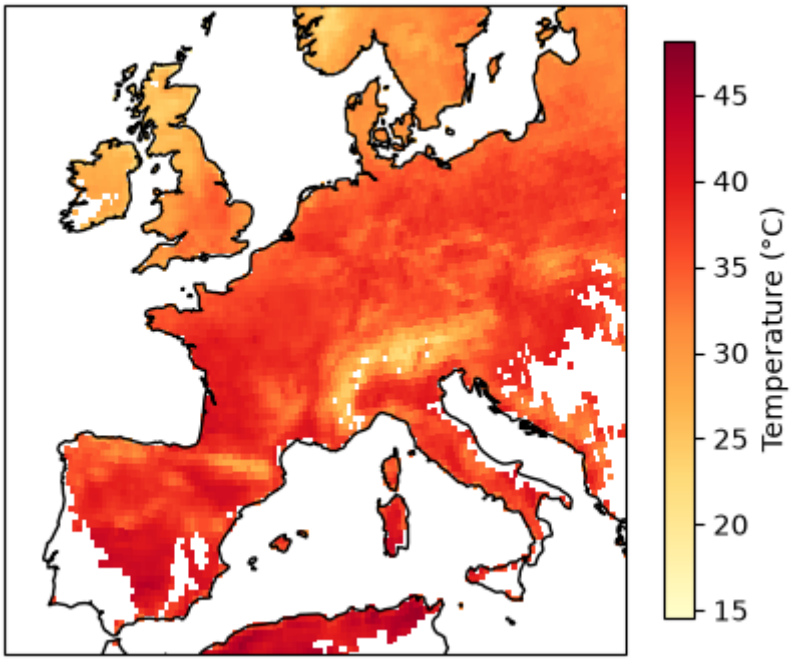

Figure A3.1: As Figure 8a, but only showing temperatures where the 2026 maximum occurred between June 22nd and 30th, during the ongoing heatwave.

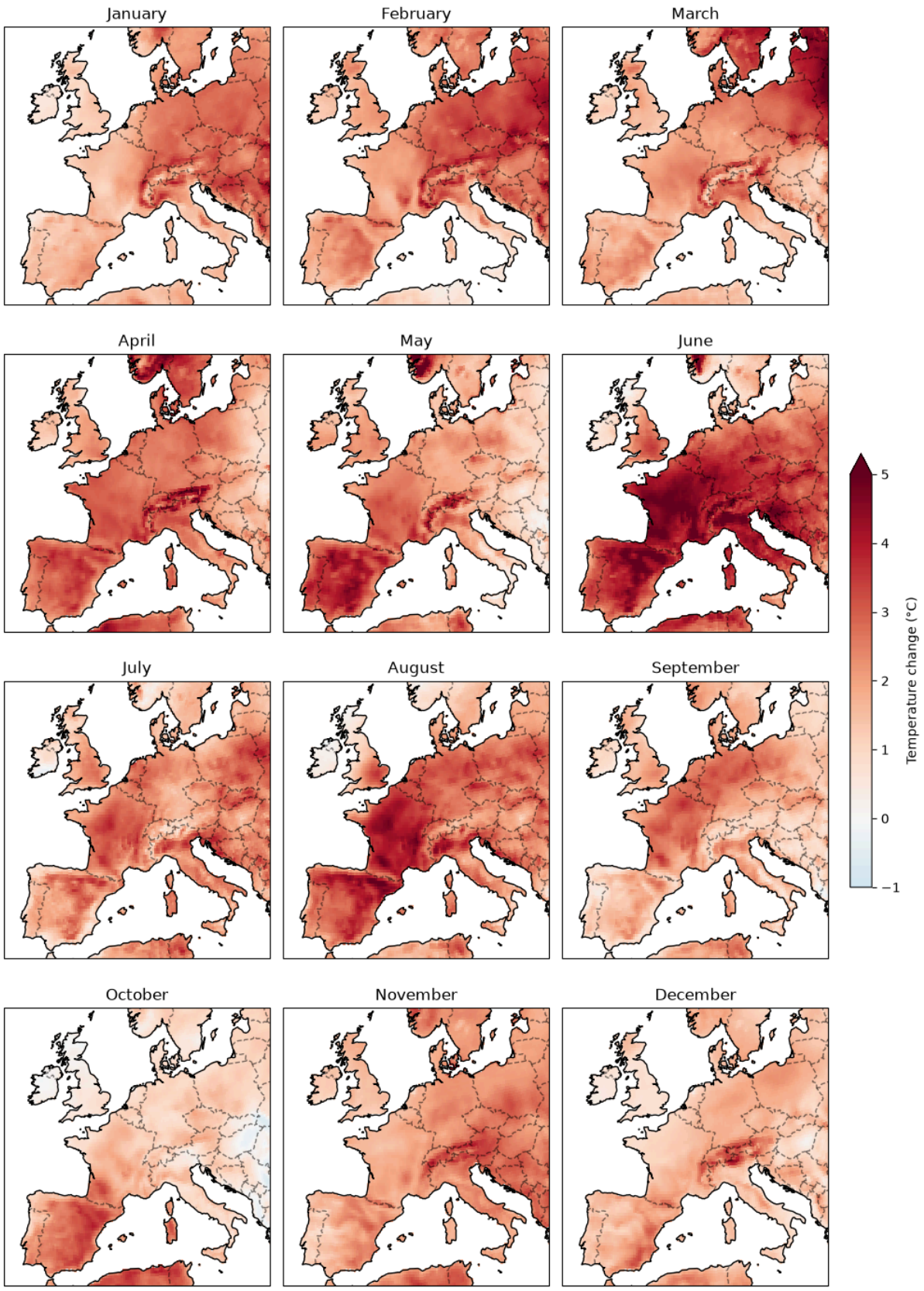

Figure A3.2: Linear change in gridwise Tx3x per degree of GMST for each calendar month, estimated using ERA5 data from 1950-2025.